Electronic Supplementary Material (ESI) for Chemical Communications.
This journal is © The Royal Society of Chemistry 2017

Supporting Information

Elucidation of the elusive structure and formula of the active pharmaceutical ingredient bismuth subgallate by continuous rotation electron diffraction

Yunchen Wang,[a] Sofia Takki,[a] Ocean Cheung,[b] Hongyi Xu,[a] Wei Wan,[a] Lars Öhrström[c] and A. Ken Inge[a]

[a]Department of Material and Environmental Chemistry, Stockholm University, 106 91 Stockholm, Sweden. Email: andrew.inge@mmk.su.se

[b]School of Engineering and Physical Sciences, Heriot-Watt University, Edinburgh, EH14 4AS, UK

[c]Department of Chemistry and Chemical Engineering, Chalmers University of Technology, 412 96 Gothenburg, Sweden

Table of Contents

Experimental procedures		S3
Materials		S3
Synthesis of bismuth subgallate		S3
Stability tests in HCl		S3
Characterization		S3
Electron diffraction		S3
Sorption		S4
Results and Discussion		S4
X-ray powder diffraction		S4
Electron diffraction		S4
Rietveld refinement		S4
Sorption		S5
Table S1.	Electron diffraction refinement details	S6
Table S2.	Rietveld refinement details	S7
Figure S1.	Scanning electron micrographs of bismuth subgallate	S8
Figure S2.	X-ray powder diffraction patterns of bismuth subgallate	S9
Figure S3.	Reconstruction of continuous rotation electron diffraction data	S10
Figure S4.	Rietveld refinement plot of bismuth subgallate	S11
Figure S5.	Solvent water molecule positions in pores	S12
Figure S6.	Interatomic distances	S13
Figure S7.	Thermogravimetric analysis and differential scanning calorimetry	S14
Figure S8.	Thermodiffraction of bismuth subgallate in air heated to 300 °C	S15
Figure S9.	Thermodiffraction of bismuth subgallate in air heated to 175 °C and cooled	S16
Figure S10.	Thermodiffraction of bismuth subgallate under vacuum	S17
Figure S11.	X-ray powder diffraction patterns of bismuth subgallate after stirring in HCl	S18
Figure S12.	N_2 adsorption isotherm of bismuth subgallate recorded at 78 K	S19
Figure S13.	CO_2 and N_2 adsorption isotherm of bismuth subgallate recorded at 273 K	S19
Figure S14.	CO_2 and N_2 adsorption isotherm of bismuth subgallate recorded at 283 K	S20
Figure S15.	CO_2 and N_2 adsorption isotherm of bismuth subgallate recorded at 293 K	S20
Figure S16.	FT-IR spectrum of bismuth subgallate	S21
Figure S17.	In situ X-ray powder diffraction during synthesis of bismuth subgallate	S22
References		S23

Experimental Procedures

Materials

Bismuth nitrate pentahydrate (Merck), gallic acid monohydrate (Sigma-Alrich), bismuth (III) gallate basic hydrate (Sigma-Alrich), hydrochloric acid 37% (VWR) and Devrom® (Parthenon) were used without further purification.

Synthesis of bismuth subgallate

$[Bi(NO_3)_3]\cdot 5H_2O$ (47 mg, 97 µmol) was ground and heated with gallic acid monohydrate (50 mg, 266 µmol) and distilled water (3 mL) in a 5 mL sealed pyrex tube at 180 °C for 60 mins while being stirred. The resultant yellow microcrystalline powder of bismuth subgallate was filtered, rinsed with distilled water and ethanol, then dried in air overnight. Elemental analysis in weight %: C 20.24, H 1.95, N 0 (calc. C19.55, H 2.11, N 0 for $[Bi(C_6H_2(O)_3COOH)(H_2O)]_n\cdot 2nH_2O$). X-ray powder diffraction patterns were consistent with commercially available bismuth (III) gallate basic hydrate (Sigma-Aldrich) and a chewable tablet of Devrom® (Fig. S1).

Stability tests in HCl

100 mg bismuth subgallate was placed in 10 mL of aqueous HCl solutions of various concentrations (pH = 0, 1, 2, 3, 4 and 5). The mixtures were sealed and stirred at 37 °C for 2 hours. At pH = 0 the solid dissolved leaving a colorless solution. At pH values 2-5 bismuth subgallate remained as a yellow solid and XPD indicated no changes to its crystal structure (Figure S11). At pH = 1 the title compound remained as the predominant phase however one additional reflection at higher angles was observed in the XPD pattern.

Characterization

Fourier transform infrared spectroscopy was performed on a Varian 670-IR spectrometer (Figure S16).

Thermal analysis including TG and DSC measurements were performed on a Netzsch STA 449 F3 Jupiter with a heating rate of 5 °C min^{-1} (Figure S7).

X-ray powder diffraction data for crystal phase identification were collected on a PANalytical X'Pert PRO MPD using Cu Kα radiation with automatic divergence slits. Samples were prepared on a zero background silicon plate. An Anton-Paar XRK900 reaction chamber was used to heat samples in air or under vacuum during the diffraction experiments. Data collection for Rietveld refinement was performed at room temperature on a similar diffractometer but with monochromatic Cu $K\alpha_1$ radiation and fixed slits (Figure S4) with the sample prepared in a well.

Electron diffraction

The sample was crushed in a mortar and dispersed in absolute ethanol. The suspension was treated by ultrasonication for better dispersion. A droplet was then taken from the suspension, put on a copper grid covered with lacey carbon and dried in air. Data collection was done on a 200 kV JOEL JEM2100 LaB_6 transmission electron microscope using two strategies. For rotation electron diffraction (RED) data collection, the grid was loaded on a single-tilt tomography holder operated at ambient temperature. Data sets were collected in the tilting range of 100° to 120° with goniometer rotation steps of 2° and a beam tilt step of 0.4°. The data frames were recorded on a Gatan Orius SC200D camera with exposure times of 1 to 3 seconds. The total data collection time for the individual data sets ranged from 40 to 60 minutes.

For continuous rotation electron diffraction data collection, a cryo-transfer holder (Gatan 914) was used as a cooling holder to collect data at low temperatures. The sample was cooled to about 173 K on the holder before insertion into the microscope. It was further cooled to about 98 K in the microscope. Data collection was done by rotating the crystal continuously using the goniometer and collecting video frames of the electron diffraction patterns using a high-speed hybrid detection camera (Timepix Quad). The rotation speed was 0.45° s^{-1} and the rotation ranges of the individual data sets ranged between 90° to 100°.

Both the RED and the continuous rotation data were first processed using the RED software for initial unit cell and space group determination and visualization. The continuous rotation data were then processed using the XDS software package,[1] where the instrumental parameters (rotation axis, beam position and beam orientation), unit cell parameters, orientation matrix and intensity profiles were refined and the intensities integrated. The resultant list of hkl intensities was used as $|F(hkl)|^2$ for structure solution and refinement, which was done using the SHELX software package.[2]

Sorption

N_2 adsorption and desorption isotherms at 78 K were recorded using a Micromeritics ASAP 2020 volumetric gas sorption analyser. CO_2 and N_2 adsorption isotherms carried out between 273 K and 293 K were recorded using a Micromeritics Gemini VII 2390 volumetric gas sorption analyser. The adsorption/desorption equilibrium at a defined pressure point is reached when the change in pressure of the system falls below 0.01% within a 20 s period, with a minimum 200 s delay. Prior to gas adsorption analyses, bismuth subgallate samples were pre-treated by heating to 403 K under a slow flow (10 cm^3 min^{-1}) of dry N_2 gas for 30 minutes. Pre-treatment carried out at temperatures lower than 403 K did not fully remove the adsorbed water molecules in the material (as compared with the expected weight loss and compared with TGA results). Pre-treatment carried out at temperatures higher than 403 K, or with heating time at 403 K longer than 30 minutes, as well as in vacuum, all caused structural changes of bismuth subgallate (discussed in the X-ray thermodiffraction section).

Results and Discussion

X-ray powder diffraction

X-ray powder diffraction (XPD) data could be indexed with an orthorhombic lattice with unit cell parameters a = 8.542 Å, b = 4.668 Å, c = 23.713 Å, $\alpha = \beta = \gamma = 90°$. However, extinction conditions could not be unambiguously determined with the extinction symbols *P_na*, *P_nb* and *P_nn* appearing equally plausible. The position of the bismuth cation could be located by Superflip[3] and FOX,[4] but all other atoms could not be located in the attempts to solve the structure from XPD data. Thus electron diffraction was performed for structure determination.

Electron diffraction

The best data set was identified from the continuous rotation data sets according to its large rotation range and apparent good signal-to-noise ratio. It contains 500 electron diffraction frames, collected from a crystal of about 1 µm in size in a tilting range from -33.3° to 62.1° at a tilting speed of 0.45° s^{-1}. The total data collection time was 210 seconds.

The unit cell parameters were determined to be: a = 8.59 Å, b = 4.83 Å, c = 24.67 Å, α = 90°, β = 90°, γ = 90°. Views of the reconstructed 3D reciprocal lattice are shown in Figure S3. The reflection conditions were identified from the 2D slices *h0l*, *hk0*, *0kl* from the 3D reciprocal lattice and the space group was determined to be *Pmna*. The positions of all non-hydrogen atoms, including those of solvent molecules positioned in the pores were found in the initial structure solution. Structure refinement was performed against the electron data using anisotropic atomic displacement parameters for Bi and isotropic ones for all other atoms. The refinement converged at R_1=0.189 for 45 parameters with 1026 independent reflections (708 had $I > 3\sigma(I)$). The data collection parameters and crystallographic information are summarized in Table S1. The pore volume was determined by the SQUEEZE routine in PLATON[5] as 45 $Å^3$ per Bi^{3+} cation.

Rietveld refinement

Rietveld refinement was subsequently performed with XPD data collected at room temperature in TOPAS 5.[6] All atoms were refined with isotropic displacement parameters. The gallate ligand was modelled using a Z-matrix to constrain some of the geometry. The aromatic ring was constrained to retain 6-fold rotational symmetry and all carbon-carbon bond lengths in the ring were refined as one parameter. The entire molecule was constrained to be planar. Carbon-oxygen distances were allowed to be refined within a range of reasonable distances. As the ligand is bisected by a mirror plane, the coordinate of the center of the molecule along the a-axis was fixed to be exactly 0.5.

Lowering the symmetry of the structure using the subgroup *P*2*na* did not result in improvement in the structure solution or refinement nor were noticeable changes to the structure model observed, thus suggesting that the ligand and structure as a whole do have mirror symmetry perpendicular to the *a*-axis implying that the ligand was planar without significant rotation of the carboxylic acid groups. Distance restraints were applied only to the two solvent water molecules in the pores. Hydrogen atoms were excluded in the Rietveld refinement.

Sorption

The CO_2/N_2 selectivity of bismuth subgallate was calculated based on the single component adsorption isotherms. In this case selectivity was calculated for a hypothetical flue gas with approximately 15 vol.% CO_2, 85 vol.% N_2 and a pressure of 101 kPa. Selectivity is operationally defined by the equation below,.

$$s = \frac{(q^{CO2}/q^{N2})}{(p^{CO2}/p^{N2})}$$

Temperature (K)	CO_2/N_2 selectivity
273	54
283	30
293	33

The CO_2 adsorption isotherms were fitted using the two-sites Langmuir isotherm model in an attempt to rationalize the collected data. Where *q* refers to the quantity of gas adsorbed at partial pressure *p*, and *b* refers to the Langmuir constants.

$$q = q^{ax}\left(\frac{b^1 \cdot p}{1 + b^1 \cdot p}\right) + q^{ax}\left(\frac{b^2 \cdot p}{1 + b^2 \cdot p}\right)$$

Temperature	q_{1max}	q_{2max}	b_1	b_2	R-squared
273	0.46	0.46	0.67	0.68	0.99019
283	0.83	0.60	0.60	0.01	0.99851
293	0.83	1.26	0.43	0.002	0.99701

The *R*-squared value for the CO_2 isotherm recorded at 273 K was lower than those at 283 K and 293 K. This corresponded to the changes in the overall shape of the CO_2 isotherm (See Figure 4 in main text) between these temperatures. The increased value q_{2max} between 283 K and 293 K and the low q_{1max} at 273 K, indicated that more CO_2 adsorption sites were available at 293 K than at 283 K and 273 K. This finding further supports the hypothesis that the void space of bismuth subgallate available for gas sorption may be temperature dependent. On the other hand, it is important to note that the two-site Langmuir isotherm model is used here to get an idea of the gas adsorption behavior of bismuth subgallate. More detailed diffraction and sorption studies are required before drawing any solid conclusions. The interesting gas adsorption behavior may open up a potential application of this material in gas separation after further studies.

Table S1. Continuous rotation electron diffraction and structure refinement details of bismuth subgallate.

Crystal system	Orthorhombic
Space group	*Pmna* (No. 53)
a / Å	8.59 (4)
b / Å	4.83 (1)
c / Å	24.67 (7)
Z	4
λ / Å	0.02510
Tilt range	– 33.3° to + 62.1°
RED frames	500
Tile speed	0.45 °/second
Completeness (to 0.7 Å)	0.643
R_{int}	0.1898
Independent reflections	1026
Observed reflections	708
h	$-11 \leq h \leq 11$
k	$-6 \leq k \leq 4$
l	$-18 \leq l \leq 20$
R_1	0.1890
wR_2	0.4095
GoF	0.861
Parameters	45
Restraints	0

Table S2. Rietveld refinement details of bismuth subgallate against XPD data.

Crystal system	Orthorhombic
Space group	*Pmna* (No. 53)
a / Å	8.5422(2)
b / Å	4.66793(9)
c / Å	23.7131(4)
V / Å^3	945.54(3)
Z	4
λ / Å	1.5406
T / °C	20
ρ_{calc} / g cm^{-1}	2.958
$2\vartheta_{min}$ / °	3.01
$2\vartheta_{max}$ / °	109.98
Observations	8230
Reflections	648
Restraints	9
Constraints	7
Structural parameters	22
Profile parameters	22
R_{wp}	0.16436
R_{exp}	0.09405
GoF	1.748

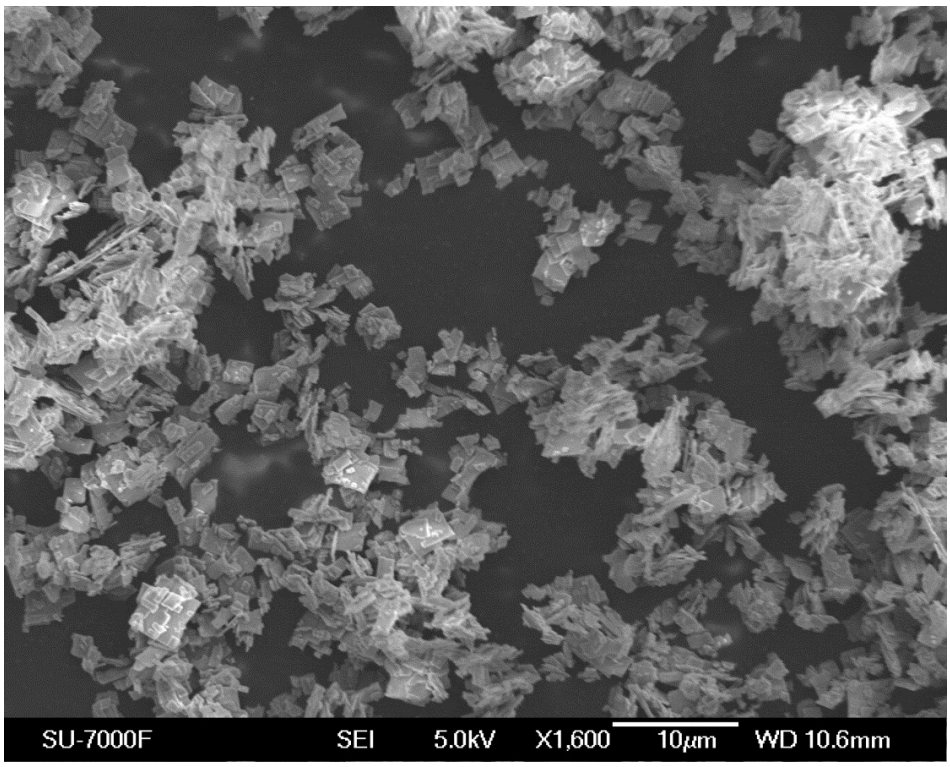

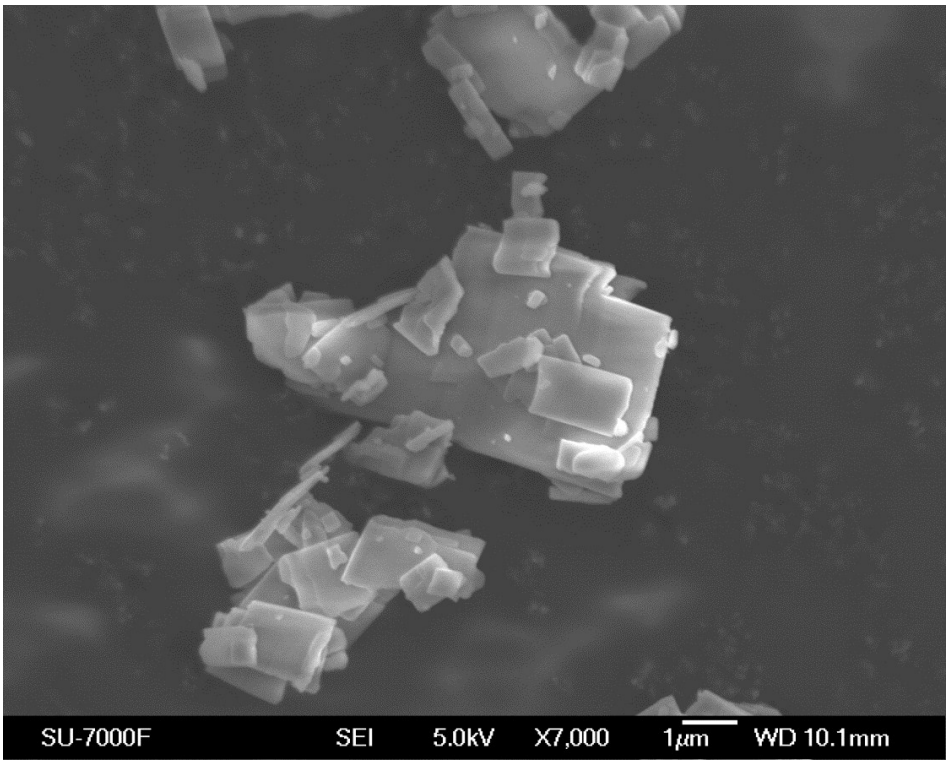

Figure S1. Scanning electron micrographs of bismuth subgallate. Crystals have plate-like morphology and are typically smaller than 6 × 4 × 0.2 μm.

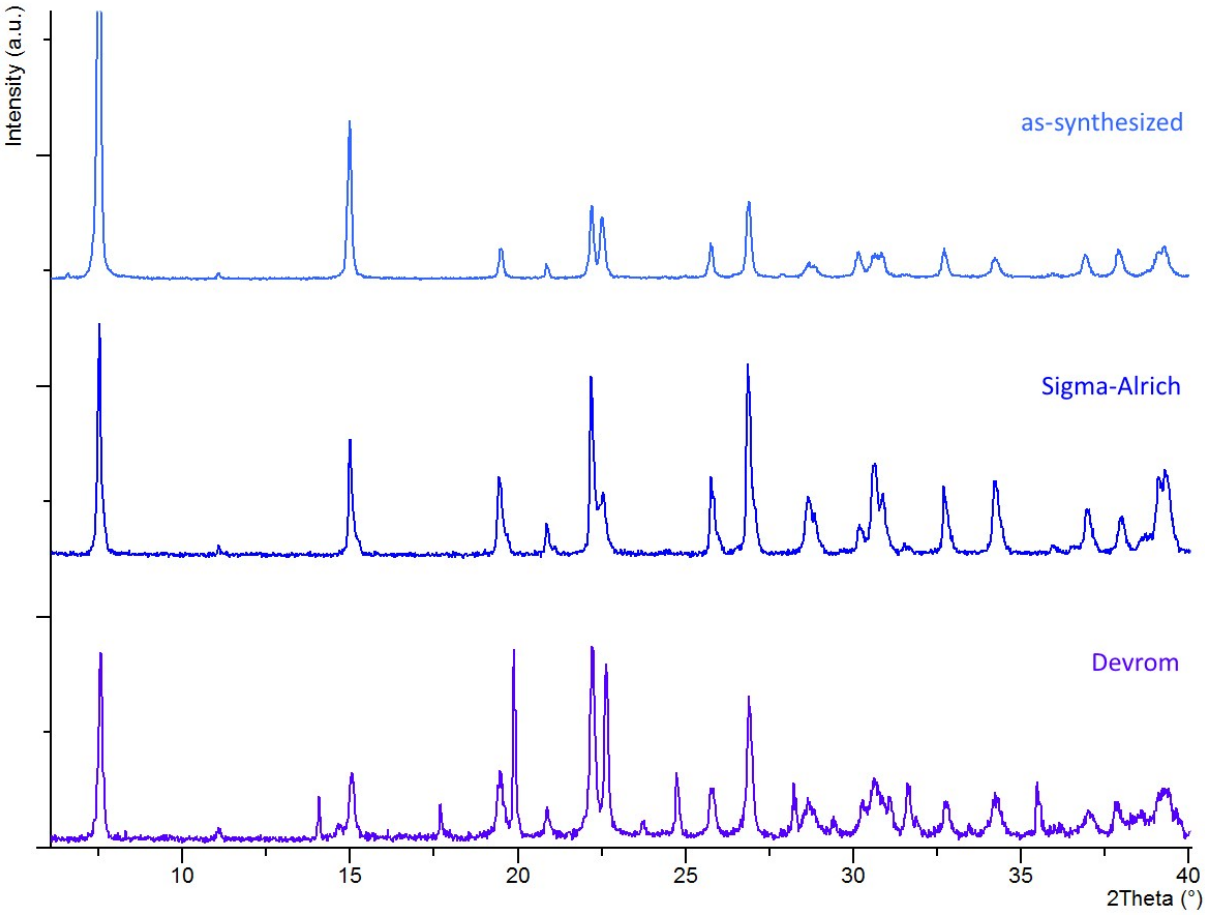

Figure S2. X-ray powder diffraction patterns of as-synthesized bismuth subgallate, bismuth subgallate purchased from Sigma-Aldrich and of a chewable tablet of Devrom®, an over-the-counter drug sold as an internal deodorant, of which the active ingredient is bismuth subgallate. Other inactive ingredients of Devrom® include magnesium stearate, microcrystalline cellulose, natural banana flavor, starch, talc and xylitol.

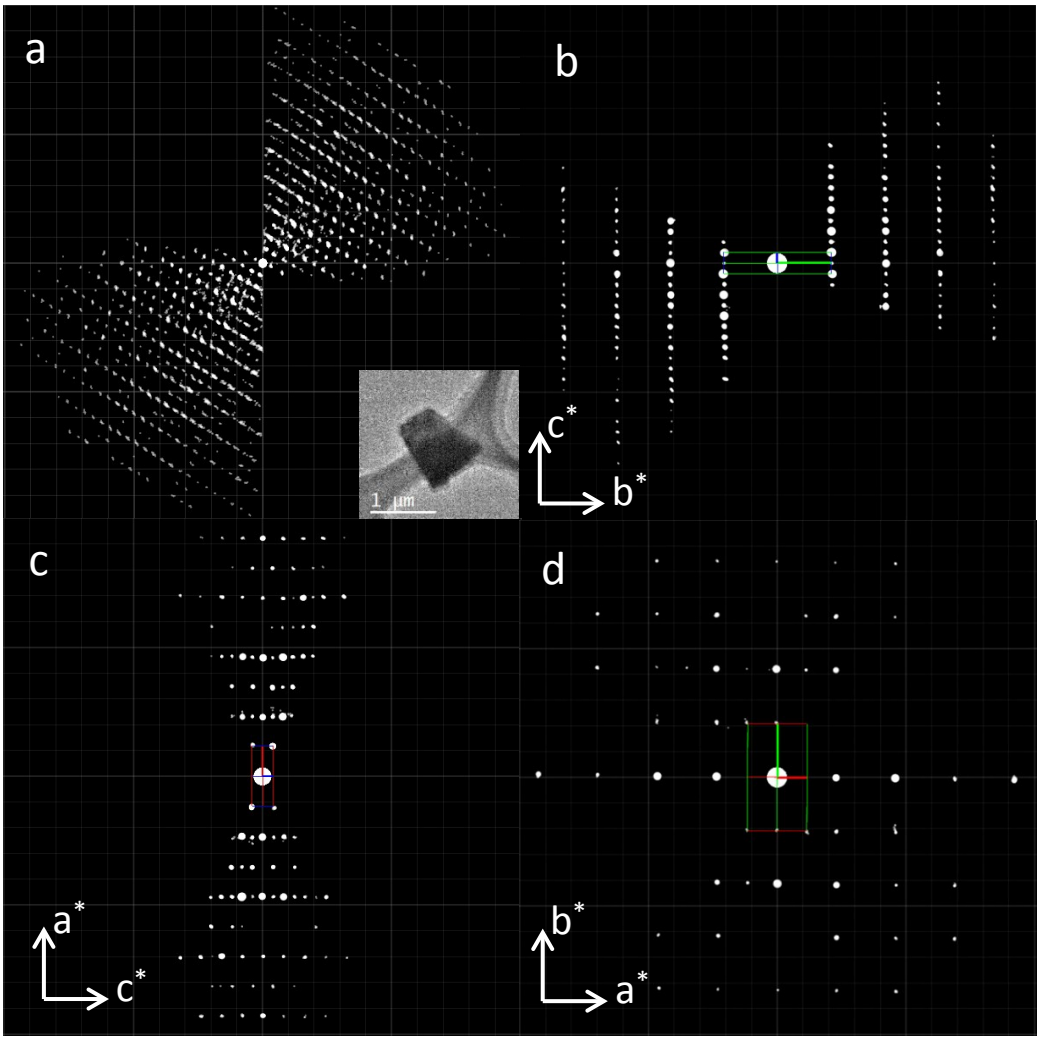

Figure S3. (a) Projection of 3D reciprocal space reconstructed from the continuous rotation electron diffraction data. The target crystal from which the data was collected is shown. The 2D slices of *0kl* (b), *h0l* (c), *hk0* (d) show the *mmm* symmetry, confirming an orthorhombic system. The red, green and blue lines indicate the *a**, *b** and *c** directions. The reflection conditions are deduced to be: *h0l*: $h + l = 2n$; *hk0*: $h = 2n$; *h00*: $h = 2n$. The space group was determined to be *Pmna*. Violations to the reflections conditions are observed in weak reflections and are due to dynamical effects in electron diffraction.

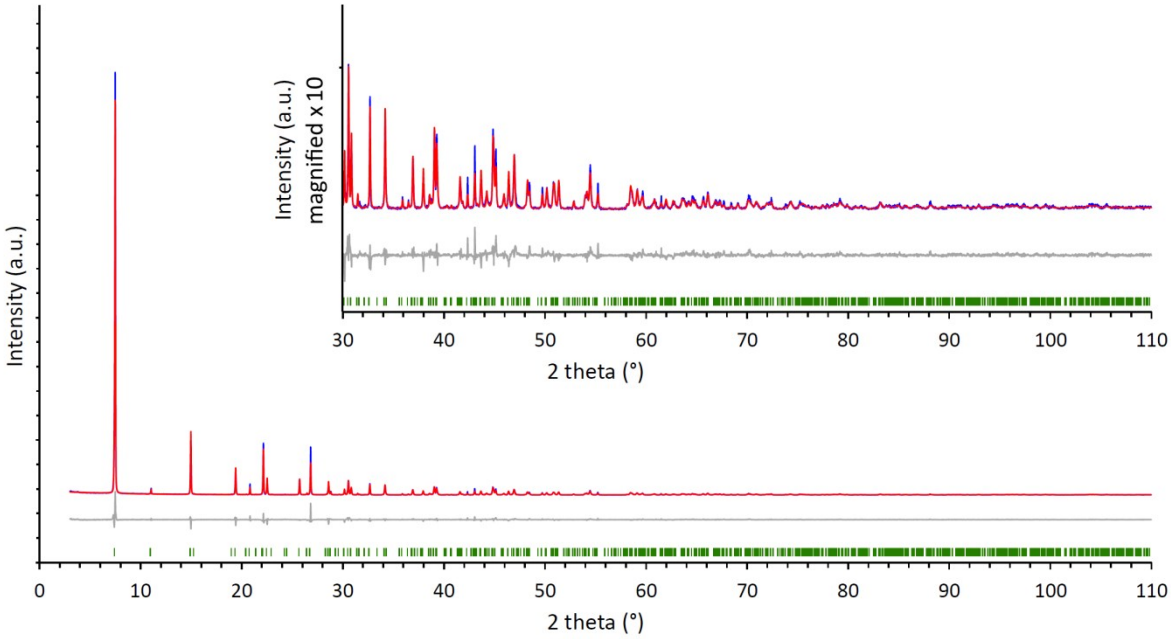

Figure S4. Rietveld refinement plot of bismuth subgallate. Observed, calculated and difference X-ray powder diffraction patterns are shown in blue, red and grey respectively. Green tick marks indicated the positions of Bragg reflections. The intensity in the region 30° < 2θ < 110° has been magnified by a factor of 10 for clarity.

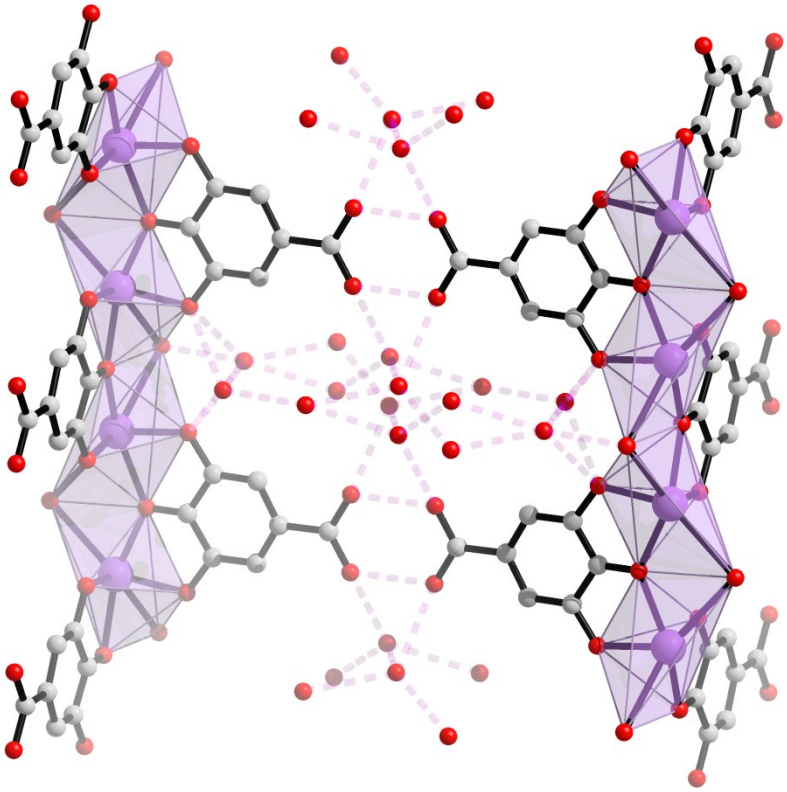

Figure S5. Positions of water molecules in the pores of bismuth subgallate. Hydrogen bonds are represented as transparent dashed magenta lines.

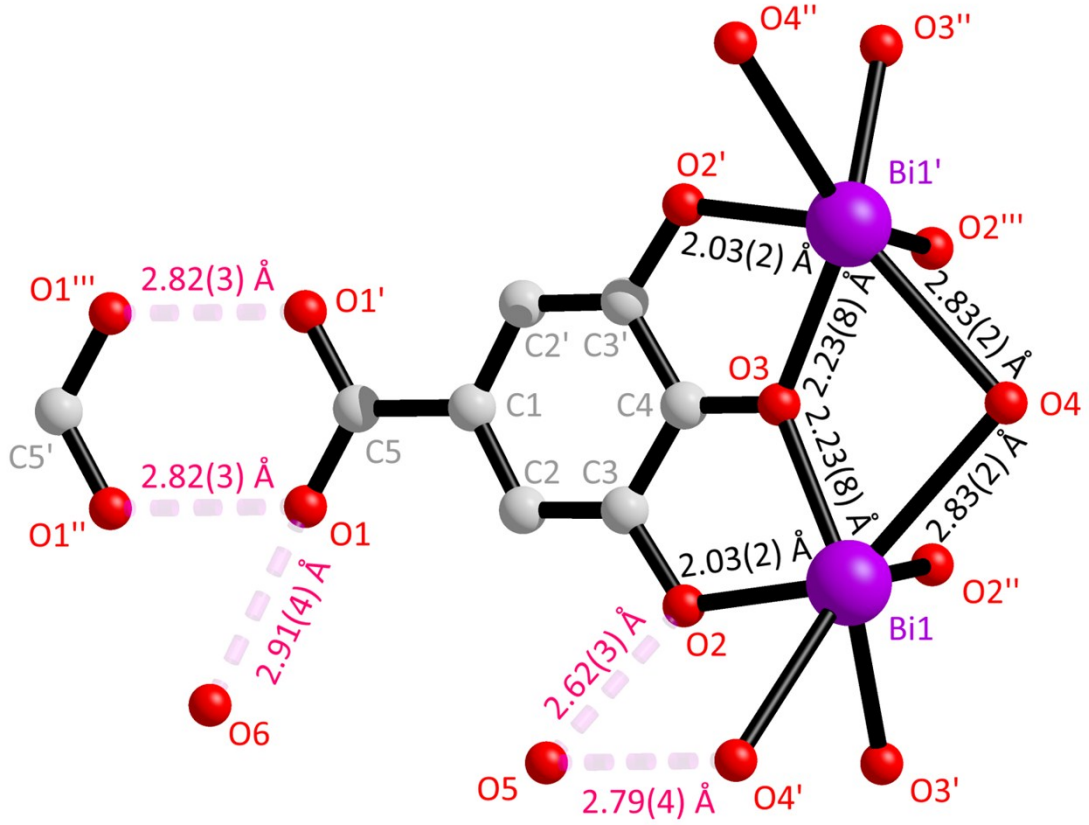

Figure S6. Select interatomic distances in the crystal structure of bismuth subgallate based on the Rietveld refinement.

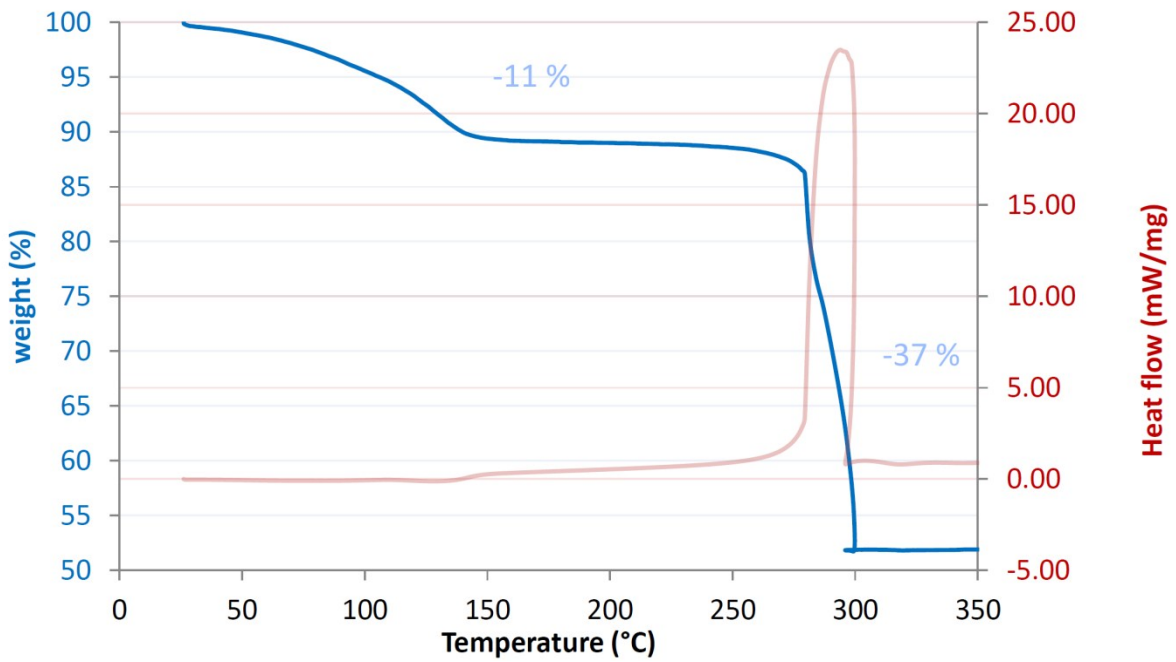

Figure S7. Thermogravimetric analysis and differential scanning calorimetry on a sample of bismuth subgallate (7 mg) heated at a rate of 5 °C min^{-1} in air. A weight loss of 11% is observed between room temperature and 150 °C which corresponds to the endothermic loss of three water molecules (calc. 12%). The discrepancy of 1% in weight loss could be due to the onset of water loss prior to the start of data collection while the sample was exposed to the air flow. A 12% weight loss was reported by Yukhin and coworkers.[7] A weight loss of 37% was observed between 260 °C and 300 °C which was attributed to the exothermic loss of the organic ligand and the formation of bismuth oxide (calc. 39%).

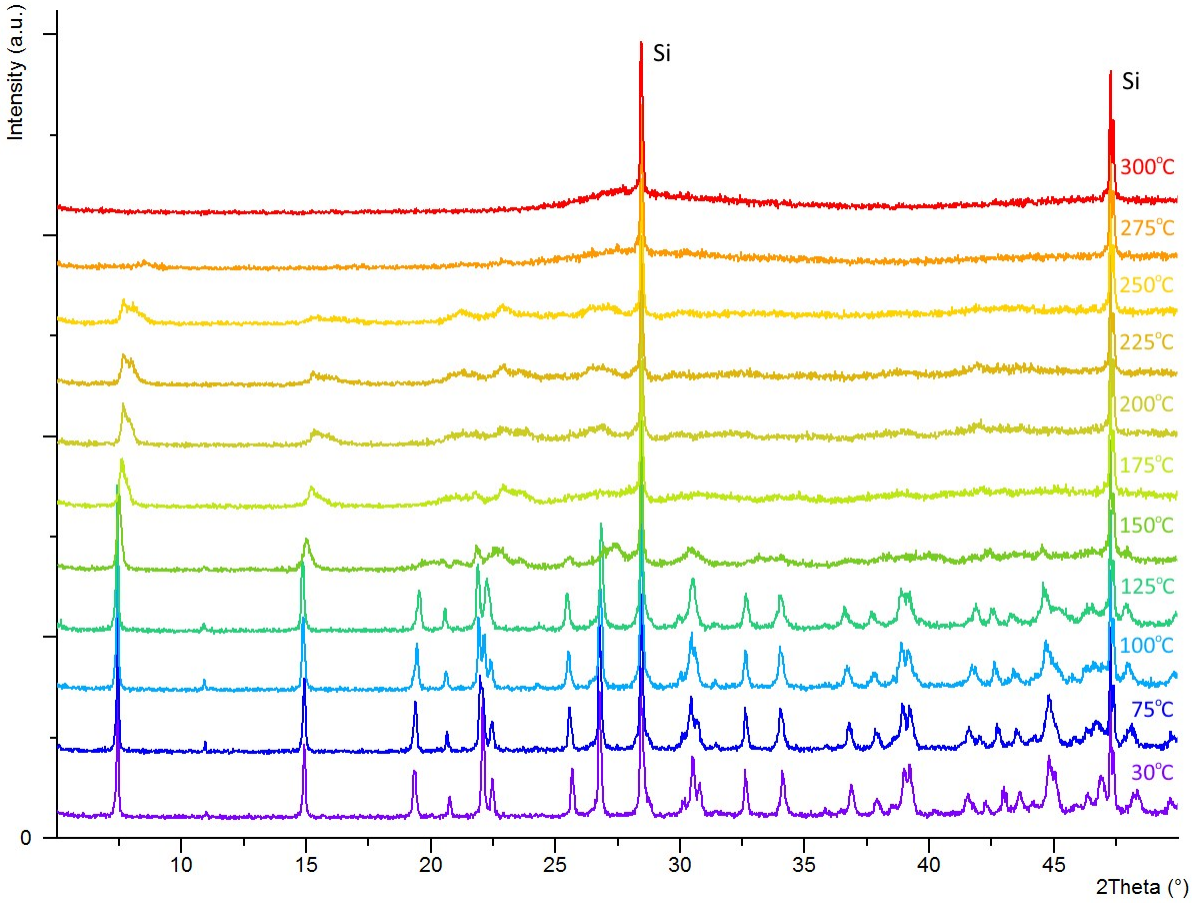

Figure S8. Thermodiffraction patterns of bismuth subgallate recorded in air with a silicon standard. Samples were heated at a rate of 5 °C min^{-1} and held at the target temperatures for 5 mins prior to X-ray powder diffraction (XPD) data collection. No significant changes were observed in the XPD patterns between 30 – 125 °C. At 150 °C many of the Bragg reflections broadened and shifted to higher 2θ values indicating partial degradation in crystallinity as well as contraction of the unit cell. The material is nearly X-ray amorphous at 275 °C which is in accord with the results from thermogravimetric analysis (TGA) which indicates loss of the organic ligand at this temperature. At 300 °C the material is completely X-ray amorphous upon completion of the loss of the organic ligand as confirmed by TGA. Bragg reflections of the silicon standard are marked.

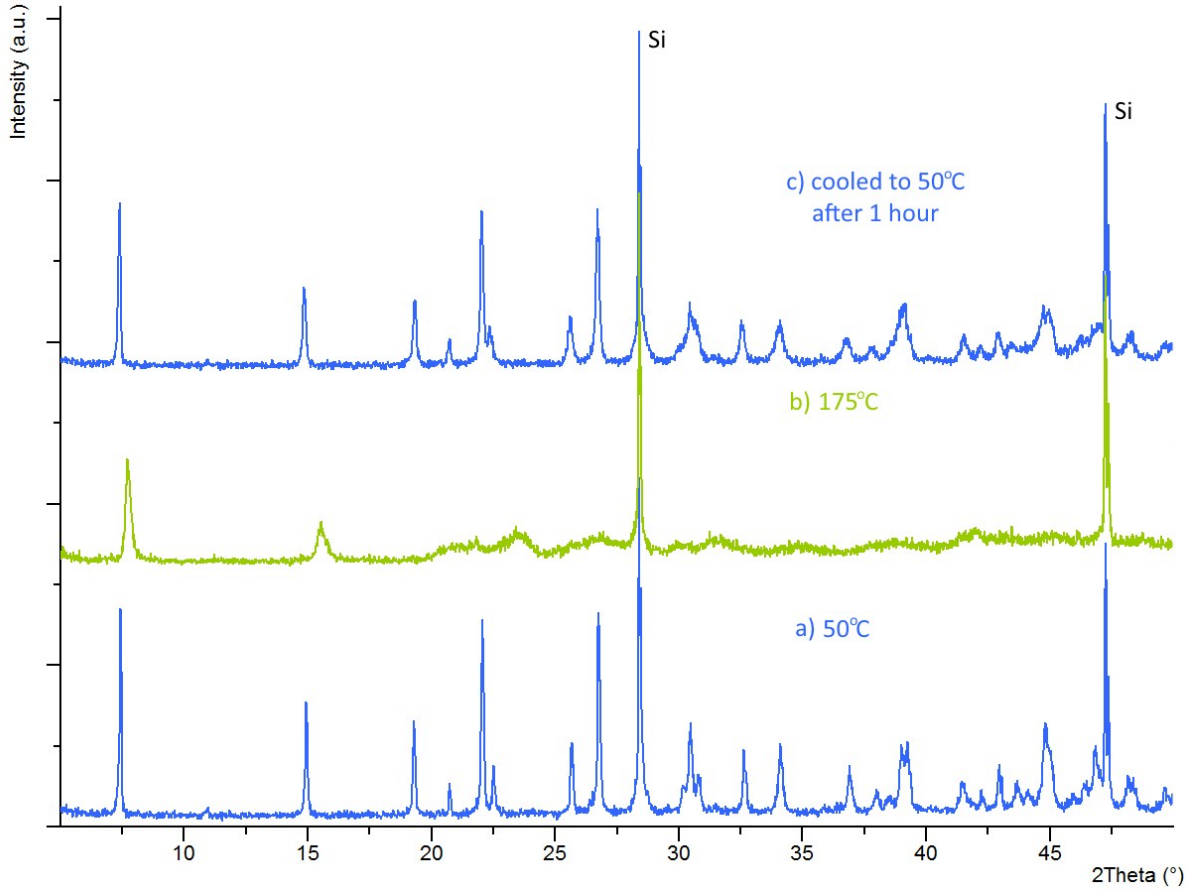

Figure S9. X-ray powder diffraction (XPD) patterns of bismuth subgallate heated in air and cooled back to room temperature. (a) XPD of the sample in air at 50 °C showing the expected XPD pattern of the highly crystalline material. (b) The sample heated in air to 175 °C showing broadening and a shift of the Bragg reflections to higher 2θ values indicating degradation in long-range order. (c) After cooling the heated sample down to 50 °C and leaving it at this temperature for one hour, the material had returned back to the original highly crystalline form, indicating a reversible structural change. Reflections from the silicon standard are marked.

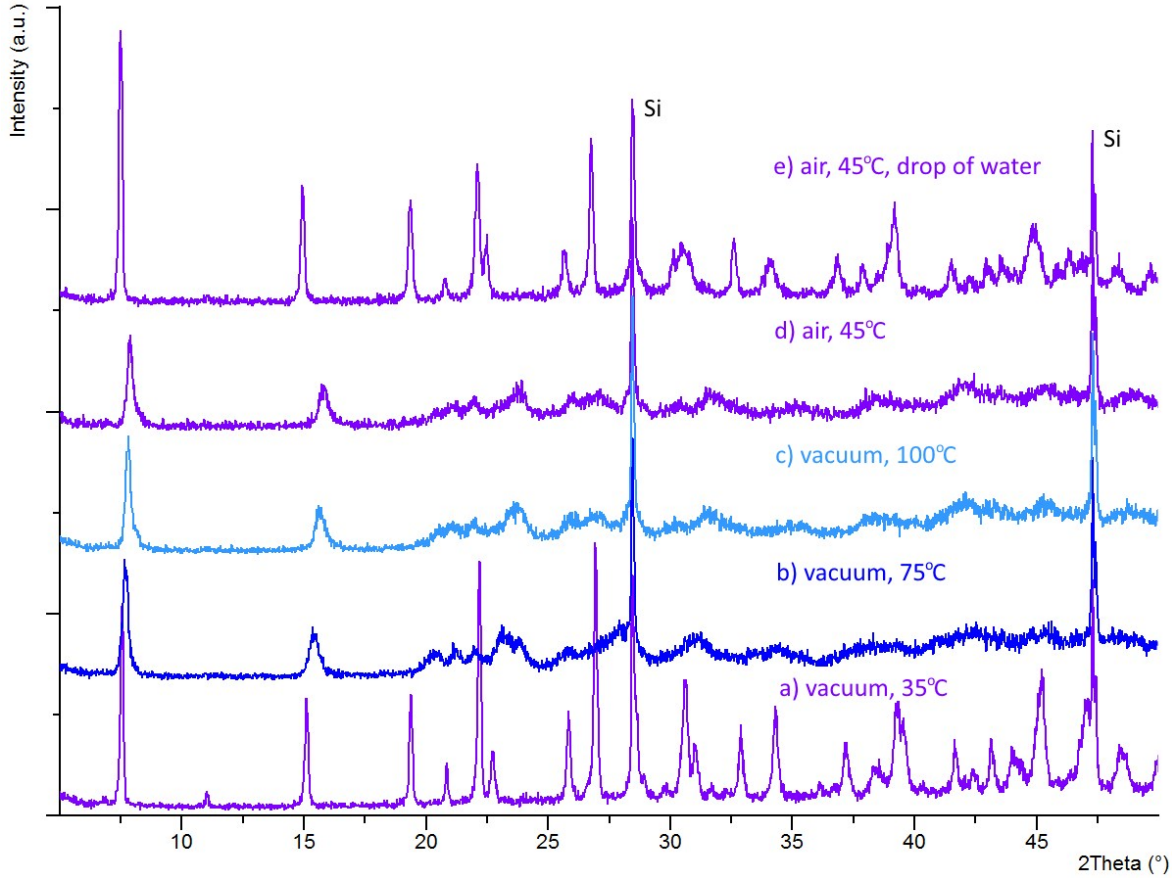

Figure S10. X-ray powder diffraction (XPD) patterns of bismuth subgallate heated under vacuum and cooled back to room temperature. (a) XPD of the sample under vacuum at 35 °C showing the expected XPD pattern of the highly crystalline material. (b,c) The sample heated under vacuum to 75 °C and 100 °C respectively showing broadening and a shift of the Bragg reflections to higher 2θ values indicating a partial degradation in long-range order. (d) After cooling the heated sample down to 45 °C the material did not immediately return back to the original highly crystalline form. (e) Placing a drop of water on the sample immediately returns the material back to its original highly crystalline form indicating that water triggers the process of returning the material back to its original form. Reflections from the silicon standard are marked.

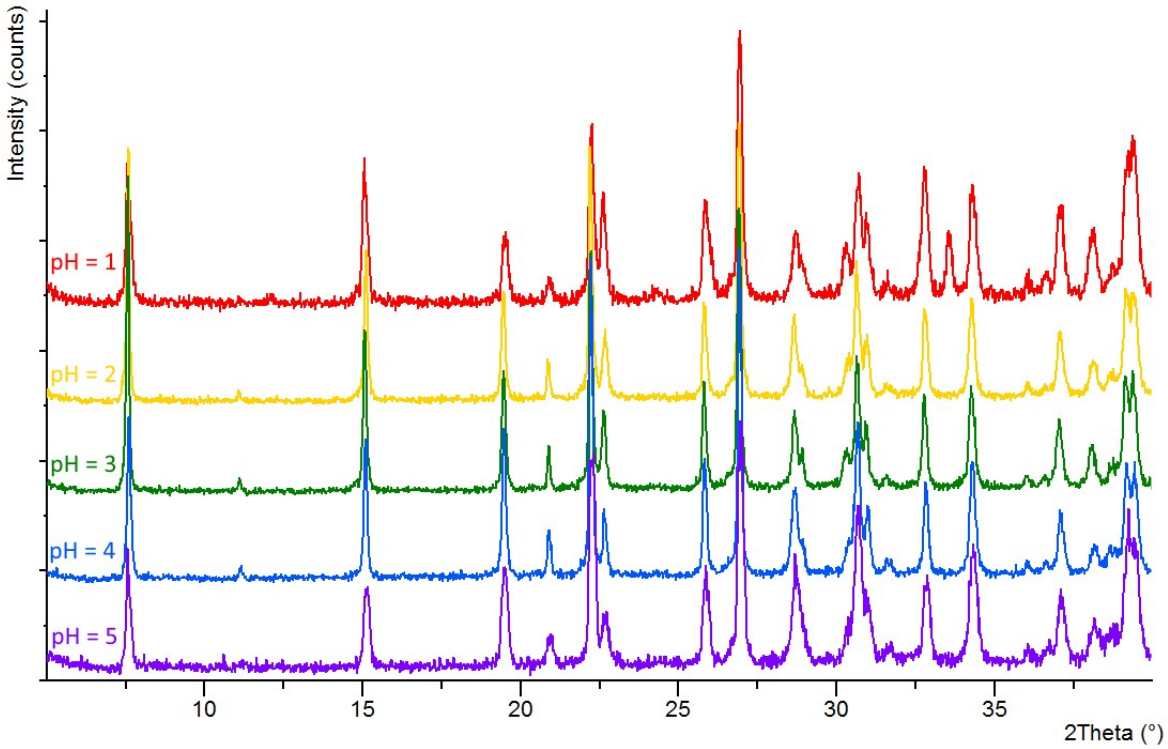

Figure S11. X-ray powder diffraction patterns of bismuth subgallate recovered after stirring in HCl at 37 °C for 2 hours. At pH = 0 bismuth subgallate completely dissolved, however at pH = 1, 2, 3, 4, and 5 bismuth subgallate remained intact. At pH =1 an additional reflection was observed at 2θ = 33.5° which suggests the presence of an additional unidentified minor crystalline phase.

Adsorption isotherms

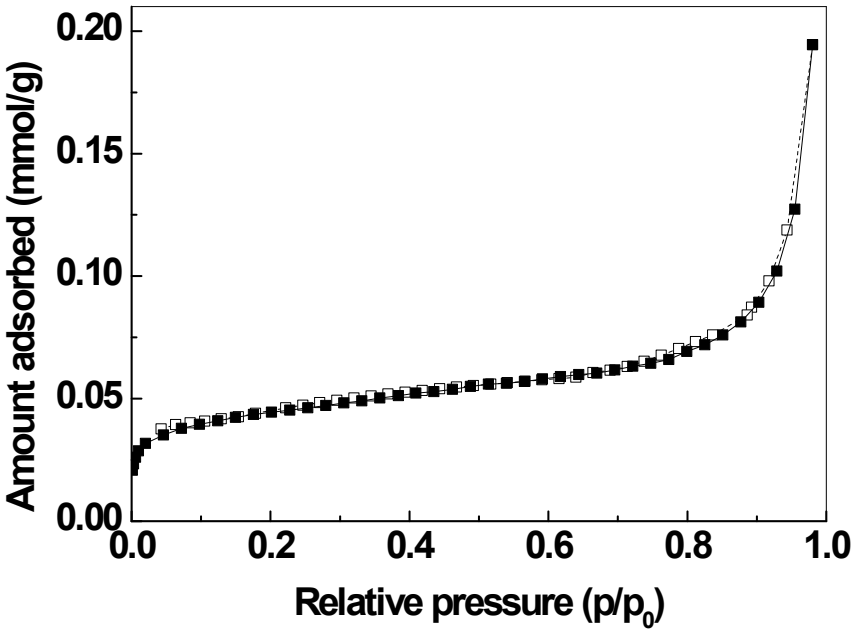

Figure S12. N_2 adsorption isotherm of bismuth subgallate recorded at 78 K.

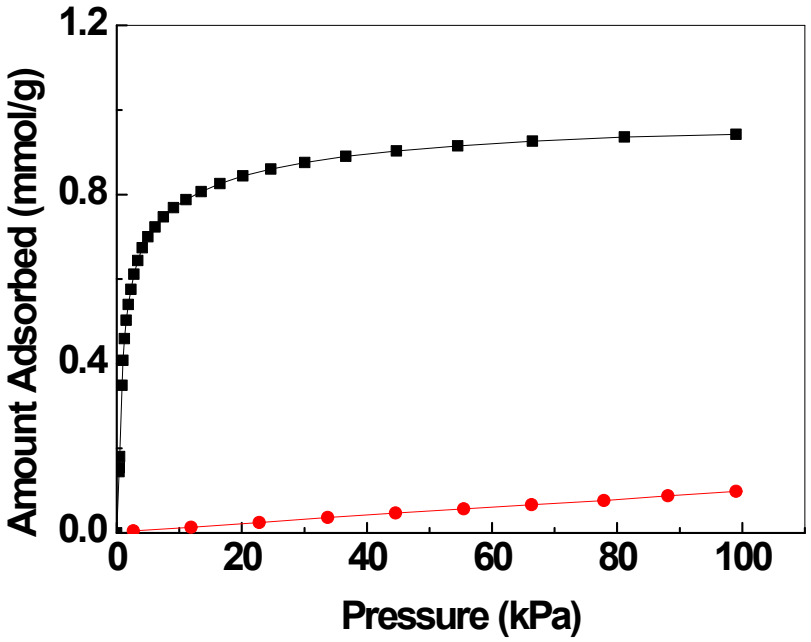

Figure S13. CO_2 (■) and N_2 (●) adsorption isotherm of bismuth subgallate recorded at 273 K.

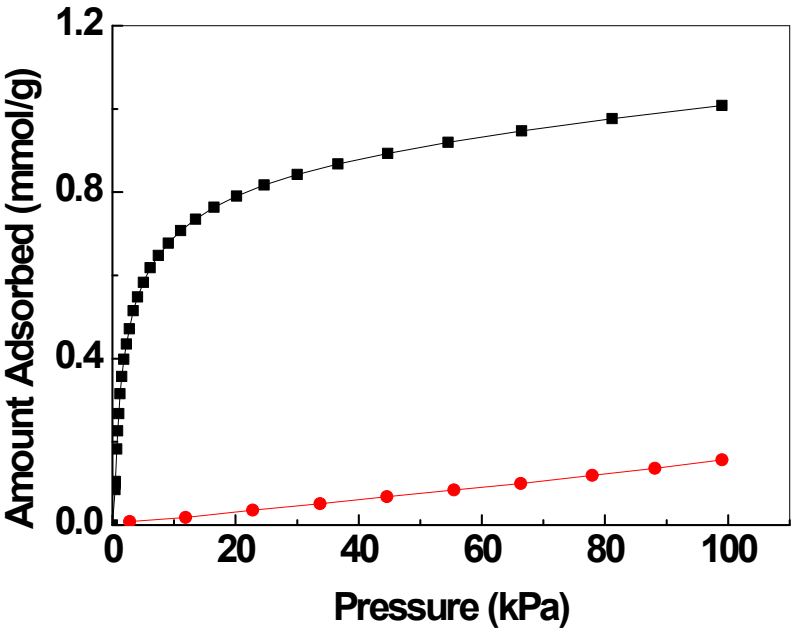

Figure S14. CO_2 (■) and N_2 (●) adsorption isotherm of bismuth subgallate recorded at 283 K.

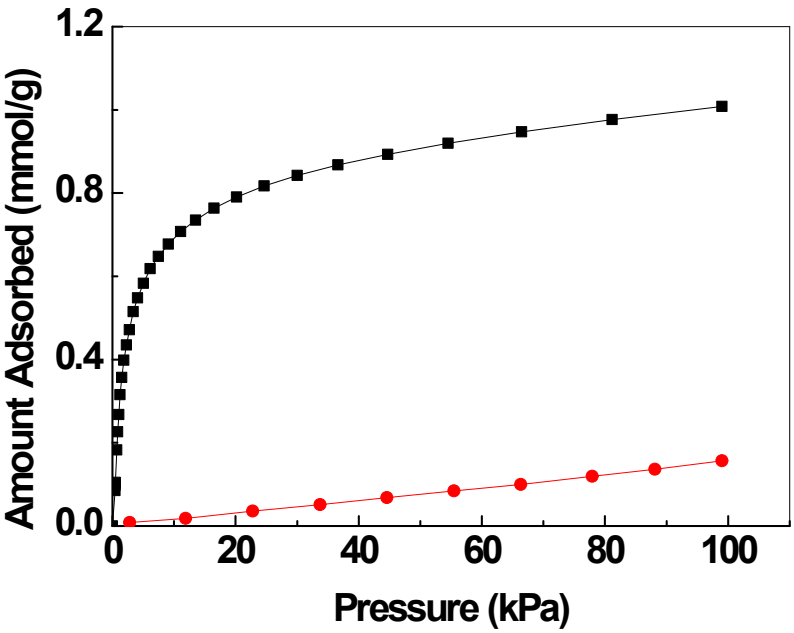

Figure S15. CO_2 (■) and N_2 (●) adsorption isotherm of bismuth subgallate recorded at 293 K.

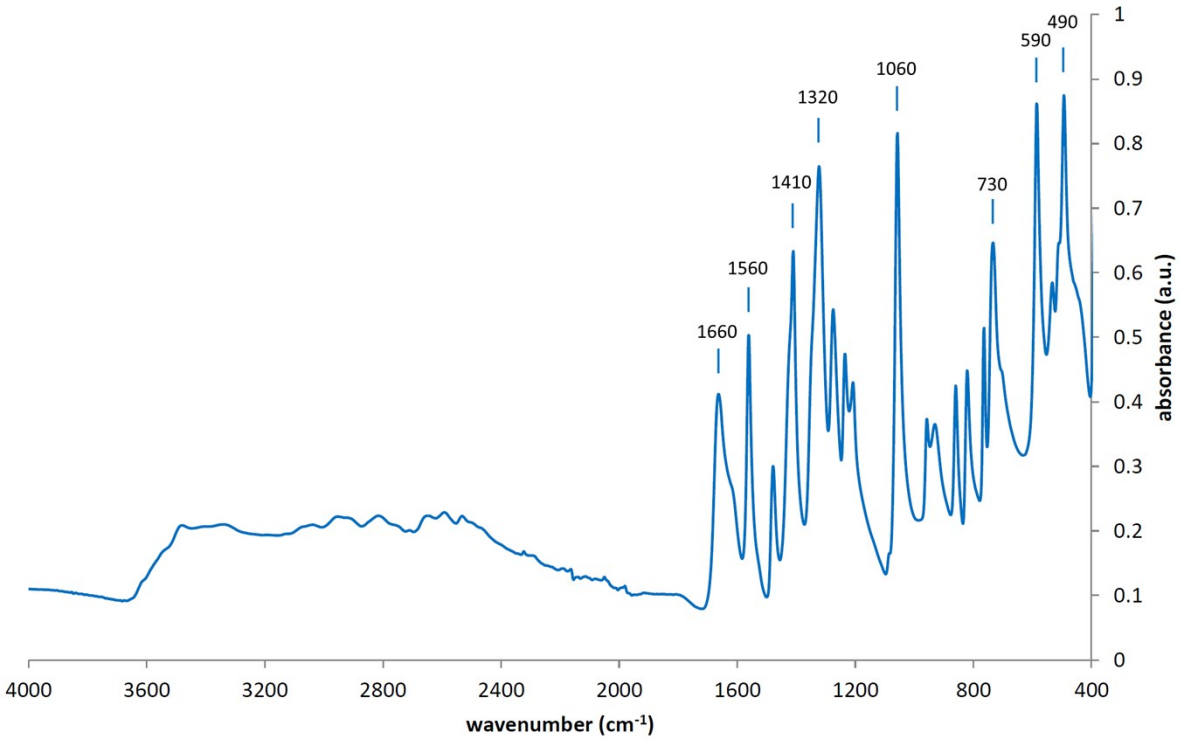

Figure S16. FT-IR spectrum of bismuth subgallate. Select absorbance bands are marked. Although the C=O stretch of carboxylic acid groups are typically observed between 1680-1750 cm^{-1} this band is shifted to lower wavenumbers when carboxylic acids are conjugated with aromatic rings and if they form dimers involved in strong hydrogen bonds with one another which weaken the C=O bond, in this case to 1660 cm^{-1}.

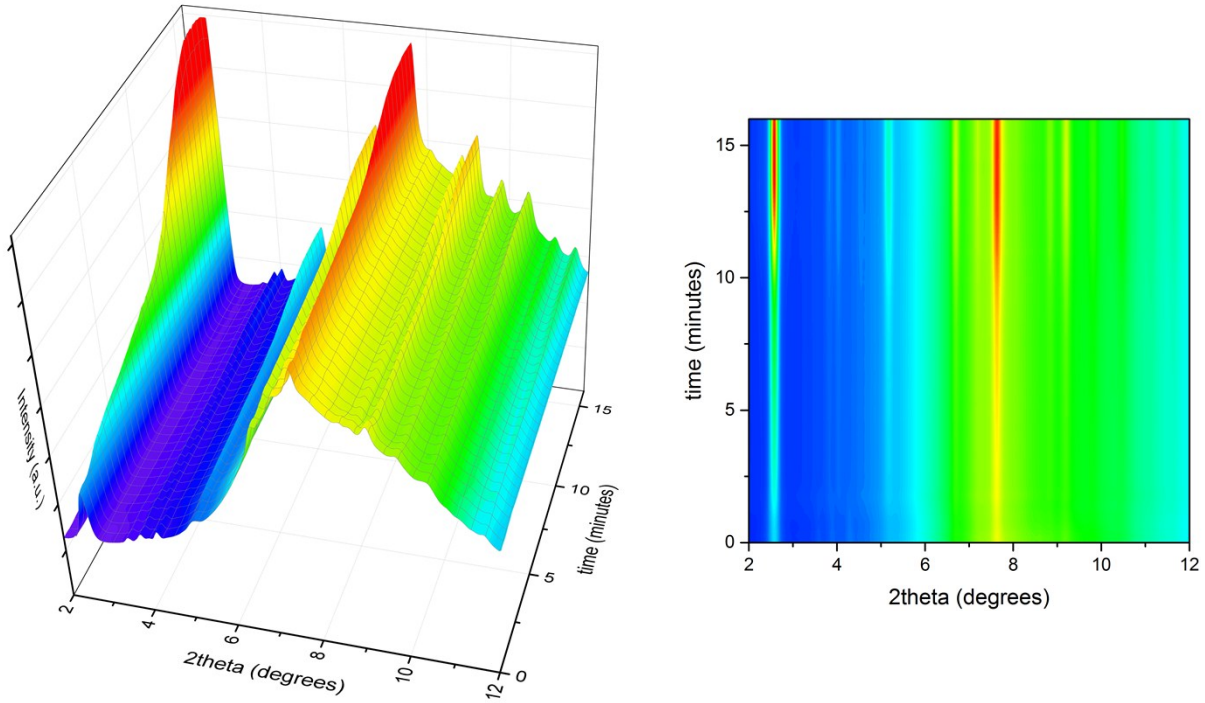

Figure S17. *In situ* X-ray powder diffraction data collected during the synthesis of bismuth subgallate using a custom-made reactor. Data were collected every 10 seconds at the beamline P09, PETRA III, Hamburg, Germany on a Perkin-Elmer XRD1621 Flat Panel detector (λ = 0.5635 Å). $[Bi(NO_3)_3]\cdot 5H_2O$ (47 mg, 97 µmol) was ground and heated with gallic acid monohydrate (50 mg, 266 µmol) and distilled water (3 mL) in a 5 mL sealed pyrex tube. The sample was stirred and heated to 80 °C as data collection began. The product already had started to crystallize at room temperature prior to heating as shown at the time of 0 minutes. Product formation was in fact complete after 15 minutes. The large background is caused by the solvent, water.

References

[1] W. Kabsch, *Acta Crystallogr. Sect. D. Biol. Crystallogr.* **2010**, *66*, 125-132.

[2] G. Sheldrick, *Acta Crystallogr. Sect. A: Found. Crystallogr.* **2007**, *64*, 112-122.

[3] C. Baerlocher, L. McCusker, L. Palatinus, *Z. Kristallogr.* **2007**, *222*, 47-53.

[4] V. Favre-Nicolin, R. Cerny, *J. Appl. Crystallogr.* **2002**, *35*, 734-743.

[5] A. Spek, *J. Appl. Crystallogr.* **2003**, *36*, 7-13.

[6] A. Coelho, *Bruker AXS, Karlsruhe, Germany* **2007**.

[7] Y. M. Yukhin, O. Logutenko, I. Vorsina, V. Evseenko, *Theor. Found. Chem. Eng.* **2010**, *44*, 749-754.